

Article

Mapping and Monitoring Lakes Intra-Annual Variability in Semi-Arid Regions: A Case of Study in Patagonian Plains (Argentina)

Facundo Scordo ^{1,2,*}, Vanesa Y. Bohn ^{1,2}, M. Cintia Piccolo ^{1,2} and Gerardo M. E. Perillo ^{1,3}

¹ CONICET—Instituto Argentino de Oceanografía, Florida 8000, Bahía Blanca, B8000BFW Buenos Aires, Argentina; vbohn@criba.edu.ar (V.Y.B.); mcpiccol@gmail.com (M.C.P.); gmeperillo@criba.edu.ar (G.M.E.P.)

² Departamento de Geografía y Turismo, Universidad Nacional del Sur, 12 de Octubre and San Juan, Bahía Blanca, B8000BFW Buenos Aires, Argentina

³ Departamento de Geología, Universidad Nacional del Sur, Av. Alem 1253, 2 do Cuerpo, of 202, Bahía Blanca, B8000BFW Buenos Aires, Argentina

* Correspondence: fscordo@criba.edu.ar

Received: 25 April 2018; Accepted: 28 June 2018; Published: 3 July 2018



Abstract: In arid and semi-arid regions, the climatic impact on lakes is especially critical, as they are scarce and play an important role as a primary source of the water supply. However, in some extended regions with those climatic conditions, the implementation of an in-situ monitoring program of high temporal resolution of the water resources is not possible due to its logistics and costs. Thus, developing an accurate methodology to monitor the evolution of water bodies is especially critical in these areas. For example, with remote sensing images, lake area fluctuation can be analyzed. The main objective of this study was to identify an efficient remote sensing methodology, with a temporal resolution that allows for analyzing intra-annual lake area variations. For detecting lakes area changes six Moderate Resolution Imaging Spectroradiometer (MODIS, National Aeronautics and Space Administration products) indexes and layers were analyzed and compared. We applied the methods to the Musters (deep) and Colhué Huapí (shallow) lakes, which are located in the extra-Andean Argentine Patagonia plains (semi-arid region). The MODIS products have not been accurate to detect the areal variations of the deep lake, probably because the spatial resolution of these images is not specific enough to identify the slight variation that these lakes usually have on the extension of their area. On the contrary, MODIS products have been accurate to analyze the areal changes of the shallow lake. The Colhué Huapí lake area fluctuated between 105 km² to 797 km². The Modified Normalized Difference Water Index (a combination of green and middle infrared electromagnetic spectrum), as well as two bands that include a different range of middle infrared surface reflectance (2105–2155 nm; 1628–1652 nm), were the most accurate to identify the variation of the lake area.

Keywords: monitoring; intra-annual variability; semi-arid region; lake area; MODIS satellite images

1. Introduction

Climate variability affects temperature, wind intensity, and precipitation patterns, which alter basin hydrology [1,2]. Frequently, lakes and reservoirs are located at the lowest position within a basin, collecting most of its water. Thus, water bodies usually have a high sensitivity to climate variability, which produces changes in its physical, chemical, and biological characteristics [3–6]. The climatic impact on the lakes is especially critical in the arid and semi-arid regions, since they are scarce and play an important role as a primary source of the water supply. Also, those regions are usually affected by desertification processes, defined as a deterioration process of soils, plants, and water resource through

which economically productive ecosystems lose their regeneration capacity [7,8]. Desertification is one of the most important environmental issues affecting 40% of continental areas [8]. The reduction of lakes surface area exposes the soil to wind erosion, rain, and surface runoff, leading to a desertification process [8].

In some extended regions with arid and semi-arid conditions, the implementation of an in-situ monitoring program of high temporal resolution of the water resources is not possible due to its logistics and costs. Thus, developing an accurate methodology to monitor the evolution of water bodies is especially critical in these areas.

Studies that are based on the analysis of remote sensing images allow for evaluating different aspects of hydrology and water resources over extended areas [9,10], such as soil moisture [11], floods [12], glacier recession and snow distribution [13–15], and water quality [16,17]. Also, lake area variation is studied by remote sensing [9,18]. Particularly, some studies showed that changes in lake area extension are indicators of climate variability because they reflect changes in the water balance and heat conditions [19–22].

Lake area fluctuations can be analyzed with a wide range of bands or indexes (calculated as a combination of bands) from the remote sensing images. For instance, the middle infrared (MIR, 1250–2500 nm) and the near infrared (NIR, 700–1250 nm) bands were successfully used for detecting open water surfaces from remote sensing images [10,23], due to the strong water absorption in contrast to a strong reflectance of the vegetation and soil in those ranges [24]. Sometimes, however, because of specific water characteristics, such as turbidity and the presence of aquatic vegetation, these bands alone are not enough to accurately distinguish open water surfaces [10]. Water-related indexes were, therefore, developed combining the MIR, NIR, and visible (VIS, 350–700 nm) spectral regions. Some of those indexes are: the Normalized Difference Water Index (NDWI1; [25]), which combines the Green (G, 495–570 nm) and NIR bands; the Normalized Difference Water Index (NDWI2; [26]), a combination of NIR and MIR bands; the Modified Normalized Difference Water Index (MNDWI), derived from the NDWI1, a combination of G and MIR bands [27]; the Normalized Difference Vegetation Index (NDVI), a combination of G and NIR bands [28], initially defined for vegetation studies that has been also proven useful for detecting water bodies from soils [18].

In this scenario, the Argentinean Patagonia (South America), and particularly the extra-Andean Patagonian plain, is an extended (800,000 km²) semi-arid region, where water resources are scarce. The lakes in this area, which are the largest and deepest in South America [29], play a crucial role for the local and regional population, and the developing opportunities of the area [30,31]. The impact of climate variability on water resources is especially critical for this region [32–34]. Temperature has increased while snow precipitation has decreased during the last century, producing glacier recession and regional hydrological changes [35,36]. Also, some of the lakes that were located within the extra-Andean Patagonian plains have their area dramatically reduced several times since 2000 [22,37,38], which increased the desertification processes. Desertification is the main socioecological issue in extra-Andean Patagonia [39].

Even though Patagonian lakes are highly sensitive to climate variability, there is a lack of monitoring programs collecting physical, chemical, and biological samples with a temporarily high resolution, which allows for understanding how these lakes are affected by climate variability. Most of the studies carried on over these lakes had a snapshot sampling approach to analyzing their physicochemical [40–43] and biological [44–46] conditions. Thus, it is necessary to develop a methodology to analyze intra-annual fluctuations in lakes and rivers, especially in the extra-Andean Patagonian region. The permanence of waterbodies, as well as the water supply of the population in this region, depend on river discharge that originated in the Andes, which is highly seasonal and can only be studied with methodologies of higher temporarily resolution. Such methods could lastly be used to improve the hydrological resources management.

Moderate Resolution Imaging Spectroradiometer (MODIS, National Aeronautics and Space Administration products) satellite images can be used to analyze lake area intra-annual variation

in remote regions where extreme climatic events effects over the water resources have been poorly studied. MODIS products have a low spatial resolution (250 m × 250 m; 500 m × 500 m) but a wide range of high temporal resolutions (0.5, 8, 16 days). In the Argentine Patagonia, lake area inter-annual fluctuations have been analyzed using Landsat images [22,38]. However, analyzing lake area intra-annual variation using Landsat images in this region is not possible. That is because, despite having a high spatial resolution (30 m × 30 m), the images have a low temporal resolution (16 days), present errors in the Landsat 7 images (since 2003), and they are not always useful due to a high percentage of cloud coverage. This last point is particularly important when developing a method to obtain intra-annual data in regions where precipitation is highly seasonal, such as in extra-Andean Argentinean Patagonia plains. Cloud cover is an issue during rainy months, and despite both MODIS and Landsat images are affected by cloud coverage, MODIS has a higher temporal resolution for some of its products (eight days). Thus, more images are available for MODIS than for Landsat products, and there are more possibilities to find an image without cloud coverage.

In this study, the accuracy of several indexes and layers, calculated and obtained from different MODIS products, for detecting lake area changes were analyzed and compared. The main objective was to identify an efficient remote sensing product, with a temporal resolution that allows for analyzing intra-annual variations. To be feasible and useful, the methodology must meet some strong conditions: (a) identify the presence of water bodies no matter its thickness; (b) have a minimal confusion between water bodies and other land covers; and (c) be able to separate the land cover automatically (without a supervised classification preprocessing). As an example, we have applied the methodology to the Musters and Colhué Huapí lakes, which are located in the extra-Andean Argentinean Patagonia plains, but it can be applied elsewhere as well.

Study Area

Musters (MU) and Colhué Huapí lakes (CH) (Figure 1) are the largest natural extra-Andean water bodies in the Argentine extra-Andean Patagonia plains [47]. They are located in the lower basin of the Senguer River (Figure 1). A ridge that reaches 600 m a.s.l. (oriented N-S) separates the lakes: the MU that is located on the West side and the CH on the East side. Although there is a short distance between them (less than 20 km), lakes show marked different physical and biological features.

Musters is a deep (maximum depth 38.5 m) lake, with 12 km width, and 40 km length. It has a tectonic origin with high elevations (900 m) on its western, northern, and central-east coasts. It is a mesotrophic lake, with middle levels of turbidity (Secchi disk 3.4 m, chlorophyll *a* 7 µg/L) [40] (Table 1). On the contrary, Colhué Huapí is a shallow (maximum depth 5.5 m) lake, with 23 km width, and 50 km length). Although originated by tectonic processes, it was reshaped by eolic and fluvial activity [47]. Except for the plateaus on its northern coast (500 m a.s.l.), most of the lake presents slight elevation on its shores. It is a eutrophic lake, with high turbidity (Secchi disk 0.07 m, chlorophyll *a* 17 µg/L) [40]. The physical differences between the two lakes are important in a period of water shortage since the shallower lake area decreased up to 80% of its mean size, while MU lake area varied less than 5% (22, 37) (Table 1).

The main tributary of both lakes is the Senguer River, which originates at the Andes (Figure 1). The Senguer River has its peak flow during spring (September–December) due to snow-melted water at the upper basin [48]. Senguer River mean discharge is 52 m³/s and it fluctuates inter-annually between 29 and 83 m³/s [49]. The Senguer River flows into the Musters Lake on its southern coast, but 50 m before reaching the lake, part of its flow diverges to the east and becomes the Falso Senguer River that discharges into the Colhué Huapí on its west coast (Figure 1). Neither of these lakes has an outflow. Thus the Senguer River basin is endorheic. Water used to flow out from the east coast of Colhué Huapí Lake through the Chico River, and finally ending in the Atlantic Ocean through the Chubut River. However, changes in climatic conditions have modified the geomorphology of the surrounding area of the Colhué Huapí Lake, and, for the last 60 years, the Chico River no longer flows [30,31,37].

Table 1. Physical and biological features of the Musters and Colhué Huapí lakes.

Lake Features	Lakes	
	Musters (MU)	Colhué Huapí (CH)
Mean depth (m)	20 *	2 *
Mean areal extension (km ²)	437 **	530 **
Maximum percentage of areal variation (%)	5 *	80 **
Trophic state	Mesotrophic *	Eutrophic *
Turbidity	Middle *	High *

Note: * [40]; ** [22].

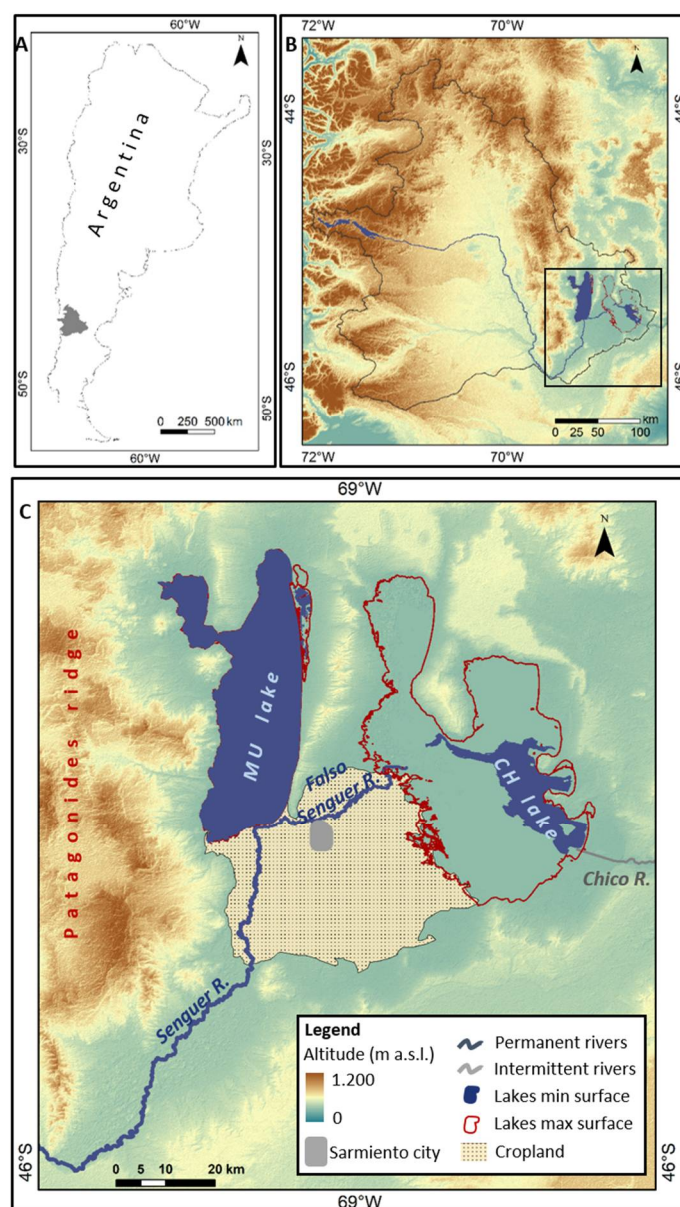


Figure 1. The study area. (A) Location of the Senguer River basin; (B) Location of the Musters and Colhué Huapí lakes; and (C) Musters and Colhué Huapí lakes. High elevations (900 m) on the western, northern and central east coasts of Musters Lake and slight elevation on Colhué Huapí shores. Maximum (red) and minimum (blue) lakes area extension obtained with Landsat images for the period 2001–2016 [22].

A series of anthropogenic impacts affect Musters and Colhué Huapí lakes. One of these impacts is the effect of agriculture. Before reaching Musters Lake, the Senguer River must pass through fertile cropland (Sarmiento Valley), which is located between the two lakes, which contain a large number of irrigation channels [37]. About 14.5 m³/s of water is used for agricultural activities during the irrigation season (July to December). The water supply for agriculture is controlled by an institution (“Instituto Provincial del Agua”) that currently has no methodology to evaluate the consequences that the water extraction produces to the two lakes. Also, Musters Lake is strategically important as a source of water for the local and regional communities (the lake supplies 150,000 m³/day of water to 254,000 inhabitants) [30].

Mean annual precipitation over the lakes is 100–200 mm/a, and it is concentrated on winter months (May to August) [50]. Mean annual temperature is 8 °C with large thermal amplitudes (>50 °C). The wind is a significant meteorological factor, with a prevailing W and SW direction, 30 km/h speeds, and gusts of 100 km/h [30]. Evaporation in this region is high (1800 mm/a).

Lake area fluctuation is related to the lake inflows (Senguer River discharge and local precipitation) and outflows (evaporation from the lakes), which are affected by two southern climate modes: El Niño–Southern Oscillation (ENSO) and the Antarctic Oscillation (AAO) [22]. Both meteorological phenomena are highly dynamic, and their interactions make it more difficult to predict their impact on the lakes.

The effect of meteorological variables over lake area inter-annual fluctuations has been analyzed by calculating the Colhué Huapí (CH) and Musters (MU) lakes area using remote sensing images Landsat 5, 7, and 8 [22]. The images corresponded to the period 1998–2015. For both water bodies, lake area as calculated with Landsat images presented a high adjusted R² (CH = 0.86; MU = 0.74) in a standard multiple regression calculated with hydrological variables [22]. A model to predict lake area fluctuation was built based on the coefficients of the standard multiple regression. The model fit for lake area was tested using the Nash–Sutcliffe model efficiency index (NSE) (CH = 0.92; MU = 0.99) [22] and a standard *t*-test for dependent samples (CH *p*-value = 0.24; MU *p*-value = 0.32; marked differences were significant at *p* < 0.01). For both of the lakes, the model calculated with Landsat images predicted their area well.

However, in the study area, it is impossible to study intra-annual changes in lakes with Landsat products. That is due to the gap of images between 2011 and 2013 (when Landsat 5 stopped working, Landsat 7 presented the strip error, and Landsat 8 was not operating), and more importantly due to the low temporal resolution of these satellites (which is critical during the winter rainy months when most of the images are not useful due to a high percentage of cloud coverage). In fact, in our study area between 2001 and 2016, it is impossible to complete a single year with one useful Landsat image per each winter month. On the contrary, with the higher temporarily resolution of MODIS products, there is at least one useful image available per month for all the years of the study period. This last point is particularly important for the future implementation of a method oriented to obtain intra-annual data in regions where precipitation is highly seasonal, such as in the study area.

2. Materials and Methods

2.1. Processing Protocol to Delineate Water Bodies

The area of CH and MU lakes were calculated using different MODIS satellite products. The images used in this study correspond to the same dates than the Landsat images that were previously used for calculating lake areas in Scordo et al. [22]. As in Scordo et al. [22], summer satellite images were used corresponding to the period 2001–2016. Also, the summer images were used because the highest river discharge occurred during spring, and its effects over the lake areal extension are more clearly appreciated during summer.

A total of 96 MODIS images were processed (16 per each band or indexes tested). The layers corresponded to MOD13Q1v6, and MOD9A1v6 products (tiles h13v13) were obtained, free of charge,

from the U.S. Geological Survey website. Each product included a series of layers. The MOD13Q1 layers used are provided every 16 days at 250 m spatial resolution. The MOD9A1v6 layers are provided every eight days at 500-m spatial resolution. The layers employed to calculate lake area were MOD13Q1v6 Normalized Difference Vegetation Index (NDVI) and Middle Infrared surface reflectance (MIR (b7); 2105–2155 nm); and, MOD9A1v6 surface reflectance bands 2 (NIR; 841–876 nm), 4 (G; 545–565 nm), and 6 (MIR (b6); 1628–1652 nm).

To obtain lake areas (km²), firstly all the layers were projected to Universal Transverse Mercator (UTM) coordinates using the MODIS Reprojection Tool v4.1 (https://lpdaac.usgs.gov/tools/modis_reprojection_tool). To differentiate water from other land covers the MOD9A1v6 surface reflectance bands 2, 4, and 6 were used to calculate three different water index: Normalized Difference Water Index 1 and 2 (NDWI1 and NDWI2) and Modification of Normalized Difference Water Index (MNDWI). While the layers MOD13Q1v6 NDVI, surface reflectance MIR band and MOD9A1v6 surface reflectance band 6 were also used alone (Table 2). Lake areas were obtained by unsupervised classification (IsoData method) and vectorization of the layers of each index calculated and bands employed. The method that was developed in this study is oriented to obtain intra-annual data, in an automatized procedure. An automatized processing should be objective (independent of the interpreter), repeatable for others users, robust, and exhaustive. All of those features are associated with an unsupervised classification method of satellite digital data. In this context, IsoData [51] is one of the most used clustering algorithms when working with an unsupervised classification of satellite images data [52], and it is frequently used in water resources studies to delineate and determine changes in water boundaries [53–56]. The information was processed by Envi 4.1 (ESRI) software and a Geographic Information System (GIS) (ArcGIS v10.0, (ESRI, Redlands, CA, USA).

Table 2. Indexes and layers (bands), calculated and/or obtained from Moderate Resolution Imaging Spectroradiometer (MODIS) products, used to calculated lake area extension.

MODIS Products	Index/Band	Equations **	References
MOD9A1v6	MNDWI: Modified Difference Water Index	$(G + \text{MIR (b6)}) / (G - \text{MIR (b6)})$	[27]
	NDWI ₁ : Normalized Difference Water Index	$(G + \text{NIR}) / (G - \text{NIR})$	[25]
	NDWI ₂ : Normalized Difference Water Index	$(\text{NIR} + \text{MIR (b6)}) / (\text{NIR} - \text{MIR (b6)})$	[26]
	MIR *: Middle Infrared	MIR (b6)	
MOD13Q1v6	NDVI *: Normalized Difference Vegetation Index MIR *: Middle Infrared	$(\text{NIR} + R) / (\text{NIR} - R)$ MIR (b7)	[28]

Note: * Layers of the products used which did not need to be calculated. ** Band electromagnetic range: MIR (b7): 2105–2155 nm; MIR (b6): 1628–1652 nm; NIR: 841–876 nm; R: 620–670 nm; G: 545–565 nm.

2.2. Validation

To validate which of the different MODIS bands and indexes are the most accurate to calculate the lakes area, the results that were obtained with them were compared with the lakes area, as calculated with Landsat images by Scordo et al. [22]. In that study, the results that were obtained with Landsat images proved to be highly correlated with the river discharge and climatic variables. A standard *t*-test for dependent samples was applied (marked differences were significant at $p < 0.01$) to compared the results that were obtained with the MODIS and Landsat images.

2.3. Application

An example of the application of MODIS images in the study area is presented. The most accurate MODIS layer has been used to analyze CH lake area intra-annual fluctuation between January of 2001 and 2002. That period and lake have been used because during 2001 the CH was close to disappearing [37], but at the end of 2001, the lake area recovered and increased 350% in less than a year. The CH lake area data during this period was obtained by analyzing 21 MODIS satellite images. Lake area data was correlated with the discharge data of its main tributary (the Falso Senguer River). The data of mean daily river flow (m³/s) corresponded to a hydrological station that was located in

the river (<http://bdhi.hidricosargentina.gov.ar/MuestraDatos.aspx?Estacion=12264>). The mean daily discharge was converted to daily discharge. Finally, lake area was correlated with the accumulated discharge from all days between images.

3. Results

3.1. Annual Time Series (2001–2016) of CH and MU Lakes Area

The reference samples (lake area calculated with Landsat images) analysis shows that, during the study period, the MU and CH lakes area presented inter-annual variation, which was more evident for the CH because of its geomorphology (shallower than MU) (Table 3, Figure 2). The CH mean area was 530 km² with a standard deviation of 219 km² (Table 4). The lake reached its lowest extension, 18% (105 km²) of its mean area, during 2001, while its largest extension, 141% (797 km²) occurred during 2007 (Table 3, Figures 2 and 3). The CH area fluctuated within a range over the study period, which was higher than 120 % of its mean area (Table 3). For CH, two different periods of lake area changes could be defined. From 2001 to 2007, the area increased up to reach 141% of its mean area. While from 2007 to 2016, the lake decreased up to reach 47% (251 km²) of it mean area (Table 3, Figure 2). The MU mean area was 437 km² with a standard deviation of 9 km² (Table 4). The lake reached its lowest extension, 95% (407 km²) of its mean area, during 2000. While it reached its largest extension, 104% (454 km²) of its mean area, during 2003 (Table 3). During the study period, the MU area fluctuated within a range lower than 10% of its mean area (Table 3).

Table 3. Increasing and decreasing lake area periods calculated with Landsat images (reference samples) using a red green blue (RGB) band combination (near infrared; short wave infrared; red; Landsat 5 and 7: bands 4–5–3. Landsat 8: bands 5–6–4).

Period of Lake Area	Year	Area CH (%)	Year	Area MU (%)
Increase	2001	18	2000	95
	2007	141	2003	104
	Variation	+123	Variation	+9
Decrease	2007	141	2003	104
	2016	47	2016	98
	Variation	−94	Variation	−6

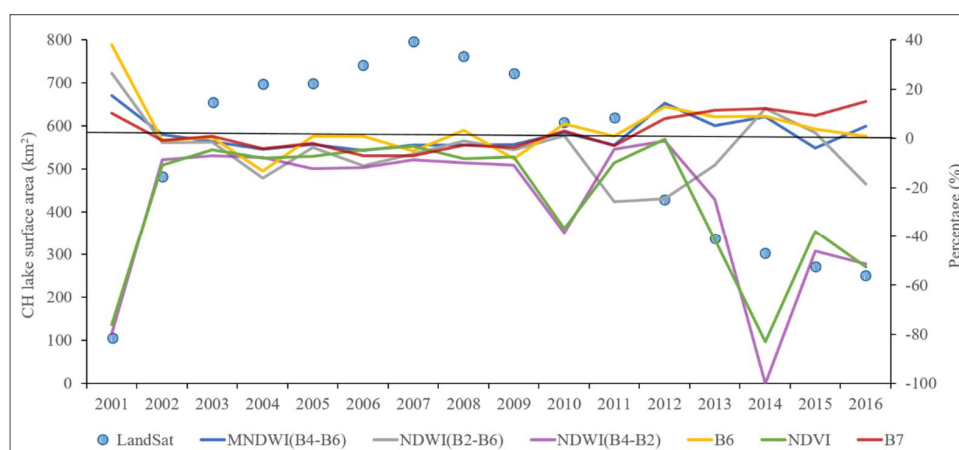


Figure 2. Colhué Huapí lakes (CH) area calculated with Landsat images (left axis). Differences (in percentage) between lake areas obtained with the MODIS (indexes and bands) and Landsat images (right axis). When lake area reached it largest extension the differences between the areas calculated with the MODIS and Landsat images is lower (e.g., 2007). The opposite occurred when lake area reached its lowest extension (e.g., 2001).

3.2. Assessment of Different Indexes and Layers Calculated and/or Obtained from MODIS Products to Calculate CH and MU Lakes Area

The time series of MU lake area calculated with all MODIS indexes and bands presented significant differences with the time series of lake area that was calculated with Landsat images ($p < 0.01$) (Table 4, Figure 4). The time series of CH lake area calculated with MNDWI, NDWI₂, MIR (b6 and b7) correlated well and do not present significant differences with the time series of lake area calculated with Landsat images ($p < 0.01$) (Table 4, Figure 4). However, time series of the lake area calculated with NDWI₂ presented significant differences with lake area being calculated with Landsat images at a $p < 0.05$ (Table 4, Figure 4). While the time series of CH lake area estimated with NDVI and NDWI₁ presented significant differences with lake area calculated with Landsat images ($p < 0.01$).

The differences between the mean value of the CH lake area time series that were obtained with the MNDWI (527 km²), MIR b6 (533 km²), and MIR b7 (529 km²), and the mean value of the lake area time series obtained with Landsat images (530 km²) are less than 0.8% (4 km²) (Table 4). Also, the differences between the standard deviation of the lake area time series that were obtained with those indexes and the standard deviation of the lake area time series obtained with Landsat images are less than 10% (24 km²) (Table 4, Figure 2).

For the CH, when analyzing annual values of lake area calculated with MODIS (MNDWI, MIR b6, and MIR b7) and Landsat images, the differences were mostly less than 10% (Figure 2). The highest inconsistencies (30–20% for MNDWI, MIR b6, MIR b7, and NDWI₂; 80% NDWI₁ and NDVI) between the lake area calculated with MODIS and Landsat images appeared in those years when the lake reached its lower extension (e.g., 2001) (Figures 2 and 3). On the contrary, when the lake area reached its largest extension (e.g., 2007), the differences between the areas estimated with MODIS and Landsat images are mostly less than 10% for all MODIS bands and indexes (Figures 2 and 3).

Table 4. Mean and standard deviation of the time series of the musters (MU) and CH areas calculated with Landsat (reference sample) and the indexes and bands calculated and/or obtained from MODIS products.

			Mean Area (km ²)	Std. Dv. (km ²)	<i>p</i>	R ²	
Colhué Huapí	Landsat (Scordo et al., 2018) *	RGB	530	219			
		MOD9A1v6	MNDWI	527	201	0.60	0.99
			NDWI ₁	435	252	0.00	0.91
			NDWI ₂	493	205	0.01	0.94
	MIR (b6)		533	202	0.74	0.97	
	MOD13Q1v6	NDVI	445	257	0.00	0.92	
		MIR (b7)	529	195	0.93	0.99	
		Musters	Landsat (Scordo et al., 2018) *	RGB	437	9	
MOD9A1v6				MNDWI	407	13	0.00
	NDWI ₁			423	9	0.00	0.76
	NDWI ₂			308	57	0.00	0.03
	MIR (b6)		420	20	0.00	0.02	
MOD13Q1v6	NDVI		429	13	0.00	0.78	
	MIR (b7)		415	10	0.00	0.04	

Note: * [22]. *p*-value of the *t*-test for dependent samples and R² values calculated between the time series of the MU and CH lakes area obtained from Landsat images, and the MODIS bands and indexes. Marked differences are significant at $p < 0.01$ (Red), while correlations are significant at R² > 0.95 (Bold).

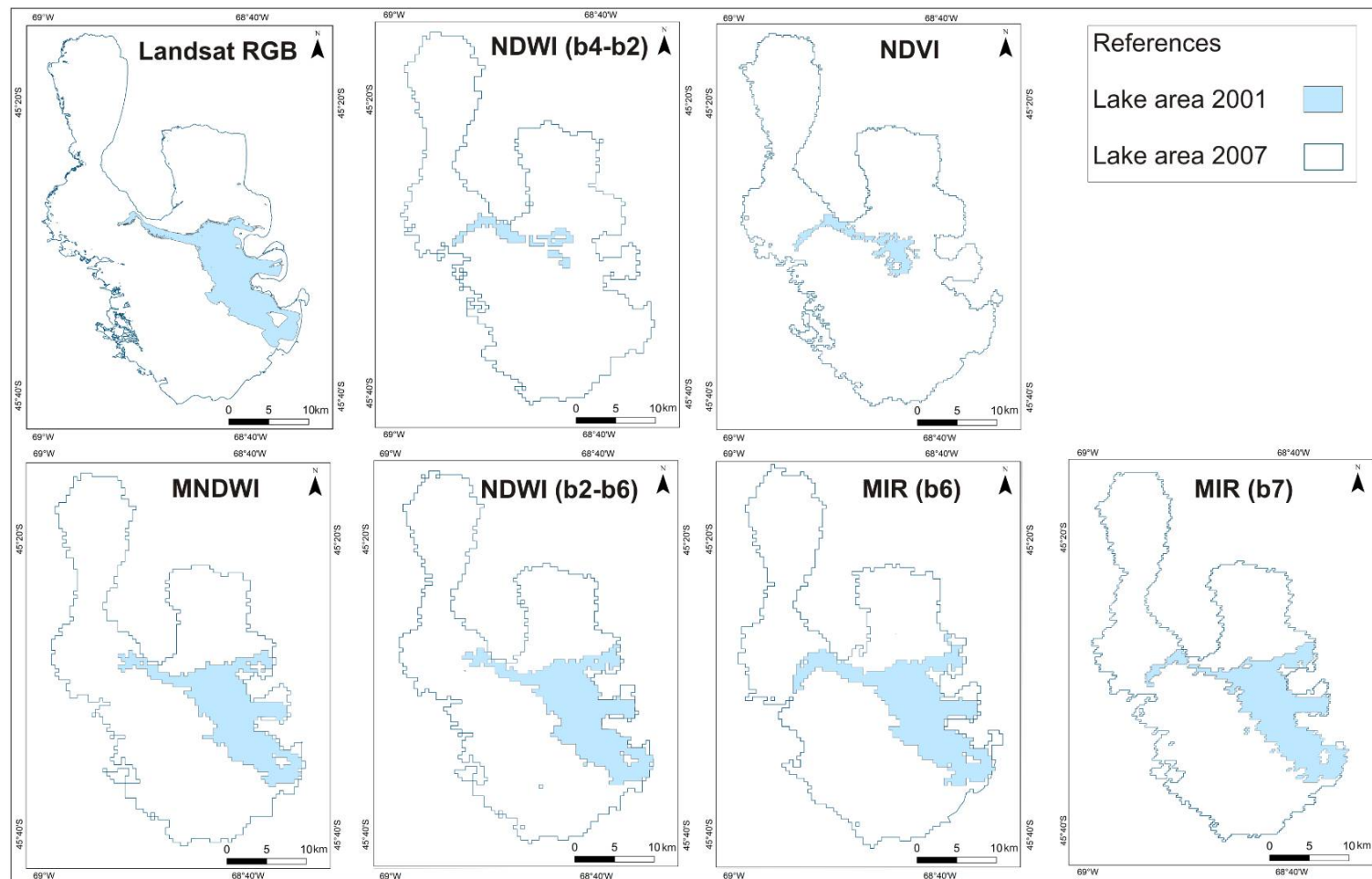


Figure 3. CH lake area calculated with Landsat and MODIS products for a year (2001) with low area extension and a year (2007) with a large area extension. On those years with low lake area extension, the Normalized Difference Vegetation Index (NDVI) and NDWI indexes produced higher errors. The errors with those indexes are probably related to the physical features of the lake. As a shallow lake soil bottom characteristics strongly influence the reflectance in the visible and near infrared domain, which are used to calculate those indexes.

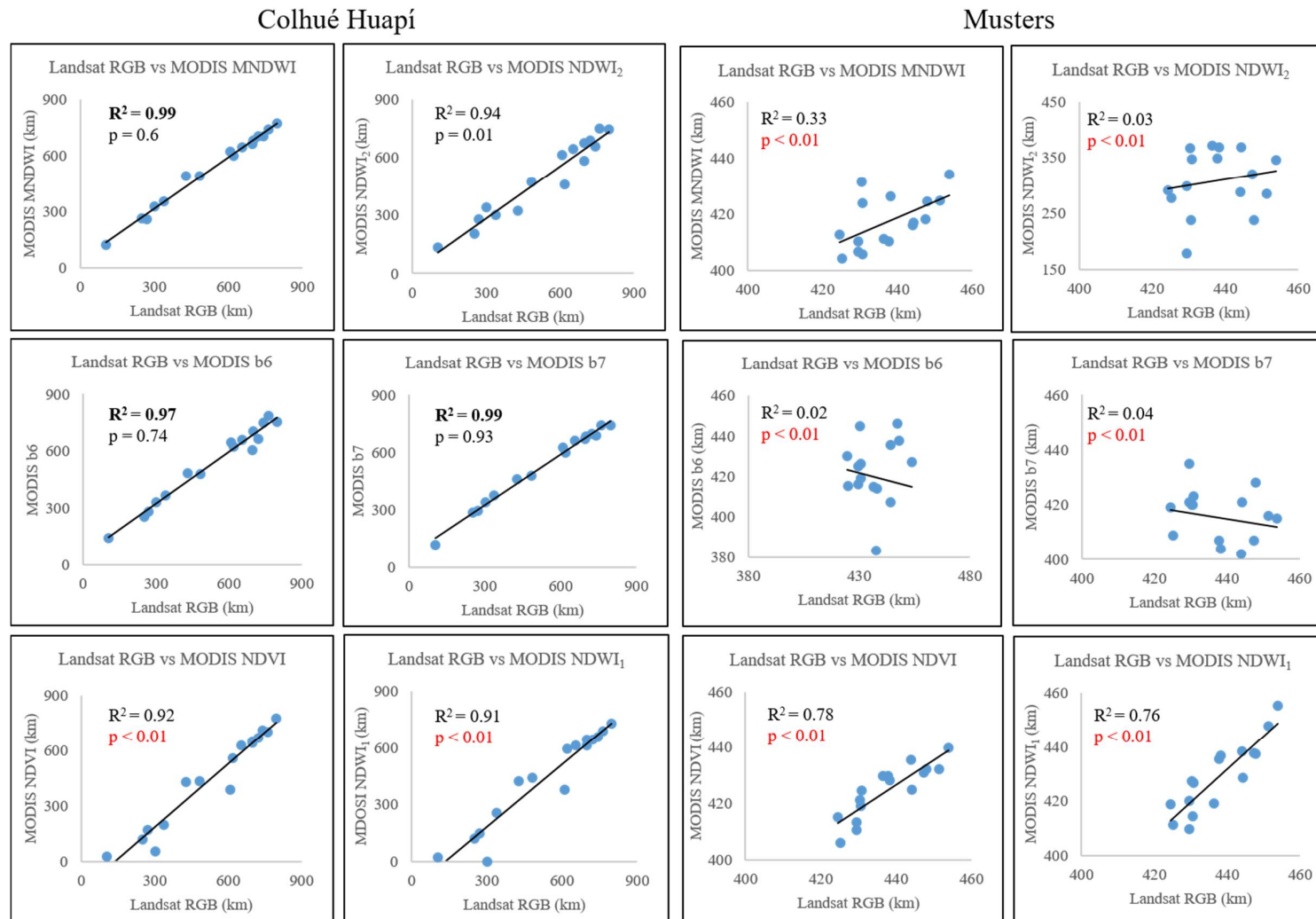


Figure 4. Scatter plots between the time series of the MU and CH lakes area obtained from Landsat images, and the MODIS bands and indexes. Marked differences are significant at $p < 0.01$ (Red), while correlations are significant at $R^2 > 0.95$ (Bold).

3.3. Application of MOD13Q1v6 MIR Band (b7)

The MOD13Q1v6 MIR band (b7) has been one of the most accurate layers to analyze the lake area variations for CH. Thus, 21 scenes of the MOD13Q1v6 MIR band were processed to analyze the CH lake area intra-annual fluctuations of between January 2001 and January 2002 (Figure 5).

Comparison of the CH lake area intra-annual fluctuations during 2001 and 2002, with the discharge values of the Falso Senguer River (CH main tributary), showed that daily discharge and lake area maximum, minimum, and periods of increasing and decreasing value, occurred on similar dates. From January to July 2001, both river discharge and lake area extension remained lower than their mean value for the period (Figure 5). On the other hand, both lake area and river discharge became higher than their mean from August to mid-December 2001, and, again, decreased from mid-December to January 2002 (Figure 5). Also, during 2001 and 2002, lake area and accumulated discharge (accumulated discharge between dates when MOD13Q1v6 images were available to calculate lake area extension) presented high correlation ($R^2 = 0.7$; $p < 0.01$).

The CH lake area fluctuated from 153 km² on 1 January 2001 to 479 km² on 1 January 2002, and its mean surface was 279 km² (Figure 5). The lake reached its lowest extension (80 km²) by 2 February 2001 and its largest extension (509 km²) by 2 December 2001. From January to July 2001, the lake area remained lower than its mean extension. While, from August 2001 to January 2002, the lake area was larger.

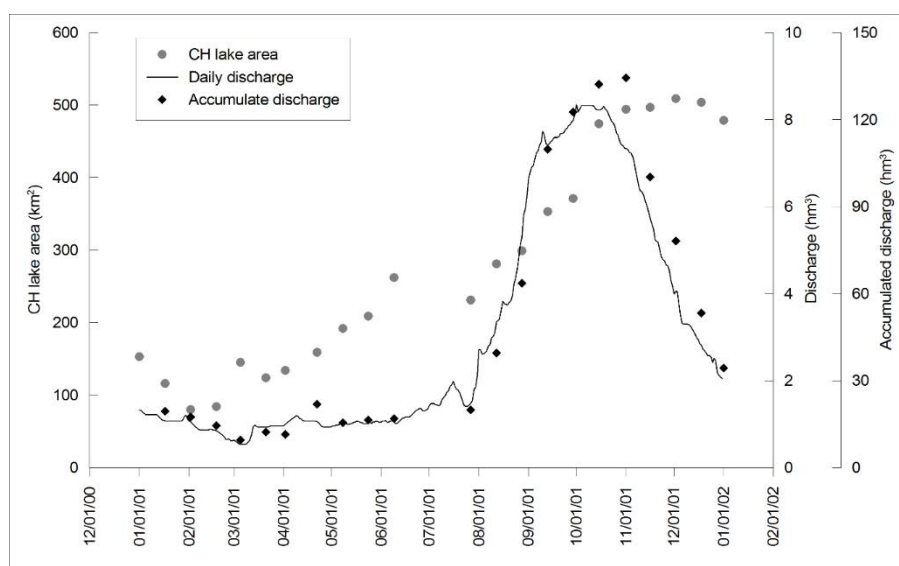


Figure 5. Comparison of the CH lake area calculated with MOD13Q1v6 middle infrared electromagnetic range (MIR) band and Falso Senguer river daily discharge from January 2001 to January 2002. From January to July 2001 the lake area and river daily discharge remained lower than their mean value for this period (279 km²; 2.7 hm³). Both lake area and river discharge stayed higher than their mean from August to mid-December 2001.

The Falso Senguer River mean daily discharge fluctuated from 0.5 hm³ on 1 January 2001 to 2 hm³ on 1 January 2002, and its mean value was 2.7 hm³ (Figure 5). The daily flow reached its lowest value (0.5 hm³) by 1 February 2001, and its highest value (8.3 hm³) by 1 October 2001. The daily discharge was lower than its mean value, from January to July 2001, and also during the last 15 days of December 2001. While daily flow was higher than its mean value from August 2001 to 15 December 2001 (Figure 5).

The CH lake area reached by 2 February 2001 was the lowest of the period 2001–2016 and that can be related to the low discharge values during January 2001 to January 2002. Falso Senguer River mean daily discharge (2.7 hm³) during January 2001 to January 2002 was 36% lower than the mean

daily flow (4.2 hm^3) of the period 2001–2016. Also, during 2001–2002 the lowest daily discharge value (0.5 hm^3) was 89% lower than the mean daily discharge of the period 2001–2016.

4. Discussion

The indexes and layers calculated and obtained from MODIS products were not accurate enough to analyze the MU lake area variations. That is probably related to the physical characteristics of the lake. The MU is a deep lake with a tectonic origin, and its area varied less than 10% (30 km^2) of its mean value (437 km^2) during the study period. A quick calculation can be done to analyze mean variation around the lake perimeter. When dividing 30 km^2 by Musters (MU) lake mean perimeter (285 km), the result is 105 m (mean variation around the lake). However, the MODIS products that were used in this study have a pixel size that is $250 \text{ m} \times 250 \text{ m}$ (MOD13Q1v6) and $500 \text{ m} \times 500 \text{ m}$ (MOD9A1v6). Thus, the lake area variations could not be addressed with the spatial resolution of MODIS images.

However, the MODIS products were an adequate tool to analyze variations in the CH lake area, which reached 120% of its mean value (530 km^2). Mean fluctuation around the lake perimeter was 1325 m . This variation could be addressed with the spatial resolution of MODIS products applied in this study. Despite having a suitable spatial resolution, not all the MODIS indexes and bands applied in this study fitted well to analyze the area variation of the CH Lake. The results that were obtained with MNDWI, NDWI2, and MIR (b6 and b7), using MODIS images correlated well and did not present significant differences with the lake area calculated with Landsat images. However, the lake area estimated with NDVI and NDWI1 using MODIS images were significantly different.

All of the indexes and layers that were suitable to analyze the CH area variations included the middle infrared electromagnetic range (MIR band). Other studies [10,23] demonstrated that the indexes using the MIR band are the most efficient for detecting water bodies in arid areas. Between the two indexes (MNDWI and NDWI2), the MNDWI, which includes a visible band and a middle infrared band in its calculation, was the most accurate (higher p-value in the T-test and higher R^2) to distinguish between water and other land covers in the study area. These results agree with those of some previous studies [23,57]. Between the two middle infrared bands, the MIR MOD13Q1v6 b7 was the most accurate to differentiate between water and other land covers. Boschetti et al. [23] explained that between MODIS MIR bands 7 and 6, the band 7 is much more sensitive to water presence but produces slightly more error (including wet soil as water) when compared with band 6. In this study, the MOD13Q1v6 b7 had a higher spatial resolution ($250 \text{ m} \times 250 \text{ m}$) than the MOD9A1v6 b6, but the former has a lower temporal resolution (16 days) than the later (eight days). Both of the bands have been proved to be useful when analyzing changes in the area of the shallow lakes. Thus, the choice to use one or another will depend on which resolution (temporal or spatial) is more important for future studies.

As in other studies [10,23,57], the indexes that do not include the middle infrared band (NDVI and NDWI1) showed a low capacity for detecting shallow water bodies. The CH is shallow, and, on these lakes, soil bottom characteristics strongly influence the reflectance in the visible and near infrared domain [23]. In our study, when the lake reached its lower extension, and consequently, the water layer was thinner, and the soil bottom had a stronger influence on the water reflectance, the differences between the results estimated with the NDVI and NDWI1, and the reference samples were 80%. While, when the lake reached its largest extension and is deeper, the differences between the areas detected with NDVI and NDWI1 and the reference samples were only 10%.

Finally, when employing 21 scenes of the MOD13Q1v6 MIR band (b7) to analyze the CH lake area intra-annual fluctuation between January 2001 and January 2002, we observed that lake area intra-annual fluctuations were correlated with river discharge values. The main river of the basin where the CH is located has its peak flow during spring (September–December) due to snow-melted water at the upper basin [48]. Consequently, the maximum values of the CH area also occurred during spring. Also, the periods where the area increases and decreases followed the patterns of the discharge.

The approach presented here allows increasing the temporal resolution in the study site from 1 to 3 (useful) Landsat images per year to 24 MODIS images per year. The MODIS images, which have a high temporal resolution, are suitable tools to analyze some natural processes that the Landsat temporal resolution does not allow. All of the previous studies that analyzed the CH area fluctuations [22,37,38] employed Landsat satellite images. Neither of them were able to estimate the intra-annual variability and to calculate a statistical relationship between the area fluctuation and other natural variables, such as river discharge. Our results allow for an entirely new approach for future studies. It would be possible to calculate multiple regressions and spectral procedures to analyze the relationship between lake area fluctuations and other natural variables, such as discharge, evaporation, and local precipitation.

As an example, in 2001, the surface area of Colhué Huapí Lake had contracted to the smallest value ever recorded (105 km²). This situation generated several issues to the regional population. Artisan fishermen from the Colhué Huapí were not able to continue fishing in this lake and needed to relocate in the Musters Lake. Also, health issues appeared due to the eolian erosion of the lake sediments [37]. Fluctuations in river discharge cause most of the Colhué Huapí Lake changes. The river discharge fluctuations can be traced back to regional climate variability and human use for agriculture [22,31]. The critical decrease in the Colhué Huapí Lake area now can be controlled with the methodology that was developed in this study. With MODIS images, it is possible to monitor the lake extent monthly with almost no budget costs. Thus, with some further analysis, the “Instituto Provincial del agua” can analyze the size of the lake and decide how much water can be available for agriculture.

5. Conclusions

The present study brings useful information to elucidate which could be the most appropriate remote sensing option for monitoring intra-annually variations in deep and shallow water bodies in semi-arid areas with highly seasonal precipitation, such as the Argentine extra-Andean Patagonia. A range of indexes and layers, which were calculated and obtained from different MODIS products, for detecting lake area changes, were analyzed and compared. The main objective was to identify the most efficient remote sensing methodology, with a temporal resolution that allows for analyzing intra-annual variations. The method must also combine the best identification of a water body (no matter its thickness), minimal confusion between water bodies and other land covers, and an automatically separation between the different land covers.

MODIS products were not accurate enough to analyze of the deep lake (MU) area variations, as the spatial resolution of these images is not detailed enough to detect the slight variation that these lakes usually have on their areal extension. On the other hand, MODIS images provide a good and relatively simple tool to analyze these variations in shallow lakes, such as CH, as their spatial resolution is high enough to detect the large variations these lakes have on their surface. In the present case, the CH lake area fluctuated within a range that was 120% of its mean surface.

Between the several indexes and bands that were tested, the Modified Normalized Difference Water Index (MNDWI) (a combination of green and middle infrared electromagnetic range), as well as two bands that include a different range of middle infrared surface reflectance (2105–2155 nm; 1628–1652 nm) were the most accurate to identify the variation of the lake area. All of those indexes and bands included the middle infrared electromagnetic range. According to these results, when analyzing the areal changes in shallow lakes in semi-arid regions, using MIR bands is suggested before incurring in the calculation of normalized water indexes. Using a band rather than the indexes allows for processing the images faster and less demanding regarding memory storage. However, if employing the middle infrared bands alone is not good enough to detect the areal changes, then calculating the MNDWI is suggested.

Unsupervised classification (IsoData) was proved to be a reliable classification methodology to detect changes in shallow lake area. We understand different mapping accuracy can be achieved using the same water index but different mapping methods [58]. In some cases, the index itself may not

sufficiently determine the accuracy of water extraction. However, in our work, we were not testing the accuracy of different mapping methods, but the accuracy of different indexes while using the same automatized mapping method. In that sense, we consider IsoData classification technic to fit the overall conditions we were looking for, it is an unsupervised, automatic, robust, objective and repeatable method. Also, the results that were obtained with this methodology were compared with lake surface area data obtained with Landsat images, which have been proved to be highly related to in-situ hydrological and climatic variable measurements [22].

Having a methodology of high temporal resolution with a base on an automatic classification to monitor lake area changes is essential in remote and poorly covered regions, like the Argentine extra-Andean Patagonia. In this region, water bodies are scarce and 254,000 inhabitants depend on them for water consumption.

Furthermore, this methodology could be employed to monitor flood events, although being a semi-arid region, it is affected by extreme precipitation events that produce high river discharges and floods. Also, this methodology has been proved to be a useful tool to monitor lakes area variations, which, when decreasing, expose soil to erosion leading to an increase of the desertification process. This is particularly important in a global context where desertification is one of the most important environmental issues, affecting 40% of continental areas. Finally, it has been shown MODIS satellite images are a powerful tool to monitoring lakes in extended regions where high temporal resolution data is needed, but there is cost restriction for environmental monitoring programs, as in Central and South America.

Author Contributions: F.S., V.Y.B., M.C.P., and G.M.E.P. designed research; F.S., and V.Y.B. performed research; F.S., V.Y.B., M.C.P., and G.M.E.P. analyzed data; and F.S., V.Y.B., M.C.P., and G.M.E.P. wrote the paper.

Funding: This research was funded by Inter-American Institute for Global Change Research (IAI) grant number CRN3038, which is supported by the US National Science Foundation (Grant GEO-1128040), and an IAI-CONICET special grant.

Acknowledgments: We would like to thank the Universidad Nacional del Sur, the Concejo Nacional de Investigaciones Científicas y Técnicas, and the project Sensing the Americas' Freshwater Ecosystem Risk from Climate Change.

Conflicts of Interest: The authors declare that the research was conducted in the absence of any relationship that could be interpreted as a potential conflict of interest.

References

1. Milly, P.C.D.; Dunne, K.A.; Vecchia, A.V. Global pattern of trends in stream flow and water availability in a changing climate. *Nature* **2005**, *438*, 347–350. [[CrossRef](#)] [[PubMed](#)]
2. Park, J.H.; Duan, L.; Kim, B.; Mitchell, M.J.; Shibata, H. Potential effects of climate change and variability on watershed biogeochemical processes and water quality in Northeast Asia. *Environ. Int.* **2010**, *36*, 212–225. [[CrossRef](#)] [[PubMed](#)]
3. Williamson, C.E.; Dodds, W.; Kratz, T.K.; Palmer, M.A. Lakes and streams as sentinels of environmental change in terrestrial and atmospheric processes. *Front. Ecol. Environ.* **2008**, *6*, 247–254. [[CrossRef](#)]
4. Williamson, C.E.; Saros, J.E.; Vincent, W.F.; Smol, J.P. Lakes and reservoirs as sentinels, integrators, and regulators of climate change. *Limnol. Oceanogr.* **2009**, *54*, 2273–2282. [[CrossRef](#)]
5. Adrian, R.; O'Reilly, C.M.; Zagarese, H.; Baines, S.B.; Hessen, D.O.; Keller, W.; Livingstone, D.M.; Sommaruga, R.; Straile, D.; Donk, E.V.; et al. Lakes as sentinels of climate change. *Limnol. Oceanogr.* **2009**, *54*, 2283–2297. [[CrossRef](#)] [[PubMed](#)]
6. Shimoda, Y.; Azim, M.E.; Perhar, G.; Ramin, M.; Kenney, M.A.; Sadraddini, S.; Gudimov, A.; Arhonditsis, G.B. Our current understanding of lake ecosystem response to climate change: What have we really learned from the north temperate deep lakes? *J. Great Lakes Res.* **2011**, *37*, 173–193. [[CrossRef](#)]
7. Mérega, J.L. El Problema de la Desertificación. In *Desertificación y Sociedad Civil*; Mérega, J.L., Ed.; Fundación del Sur: Buenos Aires, Argentina, 2003; Volume 1, pp. 11–16.

8. Mazzoni, E.; Vazquez, M. Desertification in Patagonia. In *Natural Hazards and Human-Exacerbated Disasters in Latin America*; Latrubesse, E.M., Ed.; Elsevier: Amsterdam, The Netherlands, 2010; Volume 17, pp. 351–377. [[CrossRef](#)]
9. Peng, D.; Xiong, L.; Guo, S.; Shu, N. Study of Dongting Lake area variation and its influence on water level using MODIS data. *Hydrol. Sci. J.* **2005**, *50*, 31–44. [[CrossRef](#)]
10. Soti, V.; Tran, A.; Bailly, J.S.; Puech, C.; Lo Seen, D.; Bégue, A. Assessing optical earth observation systems for mapping and monitoring temporary ponds in arid areas. *Int. J. Appl. Earth Obs. Geoinf.* **2009**, *11*, 344–351. [[CrossRef](#)]
11. Moran, M.S.; Peters-Lidard, C.D.; Watts, J.M.; McElroy, S. Estimating soil moisture at the watershed scale with satellite-based radar and land surface models. *Can. J. Remote Sens.* **2004**, *30*, 805–826. [[CrossRef](#)]
12. Sakamoto, T.; Van Nguyen, N.; Kotera, A.; Ohno, H.; Ishitsuka, N.; Yokozawa, M. Detecting temporal changes in the extent of annual flooding within the Cambodia and the Vietnamese Mekong Delta from MODIS time-series imagery. *Remote Sens. Environ.* **2007**, *109*, 295–313. [[CrossRef](#)]
13. Maurer, E.P.; Rhoads, J.D.; Dubayah, R.O.; Lettenmaier, D.P. Evaluation of the snow-covered area data product from MODIS. *Hydrol. Process.* **2003**, *17*, 59–71. [[CrossRef](#)]
14. Lopez, P.; Sirguey, P.; Arnaud, Y.; Pouyaud, B.; Chevallier, P. Snow cover monitoring in the Northern Patagonia Icefield using MODIS satellite images (2000–2006). *Glob. Planet. Chang.* **2008**, *61*, 103–116. [[CrossRef](#)]
15. Immerzeel, W.W.; Droogers, P.; de Jong, S.M.; Bierkens, M.F.P. Large-scale monitoring of snow cover and runoff simulation in Himalayan river basins using remote sensing. *Remote Sens. Environ.* **2009**, *113*, 40–49. [[CrossRef](#)]
16. Harma, P.; Vepsalainen, J.; Hannonen, T.; Pyhalahti, T.; Kamari, J.; Kallio, K.; Eloheimo, K.; Koponen, S. Detection of water quality using simulated satellite data and semi-empirical algorithms in Finland. *Sci. Total Environ.* **2001**, *268*, 107–121. [[CrossRef](#)]
17. Wu, M.; Zhang, W.; Wang, X.; Luo, D. Application of MODIS satellite data in monitoring water quality parameters of Chaohu Lake in China. *Environ. Monit. Assess.* **2009**, *148*, 255–264. [[CrossRef](#)] [[PubMed](#)]
18. Bohn, V.Y.; Delgado, A.L.; Piccolo, M.C.; Perillo, G.M.E. Assessment of climate variability and land use effect on shallow lakes. *Environ. Earth. Sci.* **2016**, *75*, 818. [[CrossRef](#)]
19. Shi, Y.F.; Ren, J.W. Glacier Recession and Lake Shrinkage Indicating a Climatic Warming and Drying Trend in Central Asia. *Ann. Glaciol.* **1990**, *14*, 261–265.
20. Qinghua, Y.; Tandong, Y.; Feng, C.; Shichang, K.; Xueqin, Z.; Yi, W. Response of Glacier and Lake Covariations to Climate Change in Mapam Yumco Basin on Tibetan Plateau during 1974–2003. *J. China Univ. Geosci.* **2008**, *19*, 135–145. [[CrossRef](#)]
21. Yan, L.; Zheng, M. The response of lake variations to climate change in the past forty years: A case study of the northeastern Tibetan Plateau and adjacent areas, China. *Q. Int.* **2015**, *371*, 31–48. [[CrossRef](#)]
22. Scordo, F.; Perillo, G.M.E.; Piccolo, M.C. Effect of southern climate modes and variations in river discharge on lake surface area in Patagonia. *Inland Waters* **2018**. accepted for publication. [[CrossRef](#)]
23. Boschetti, M.; Nutini, F.; Manfron, G.; Brivio, P.A.; Nelson, A. Comparative Analysis of Normalised Difference Spectral Indices Derived from MODIS for Detecting Surface Water in Flooded Rice Cropping Systems. *PLoS ONE* **2014**, *9*, e88741. [[CrossRef](#)] [[PubMed](#)]
24. Verdin, J.P. Remote sensing of ephemeral water bodies in Western Niger. *Int. J. Remote Sens.* **1996**, *17*, 733–748. [[CrossRef](#)]
25. McFeeters, S.K. The use of the normalized difference water index (NDWI) in the delineation of open water features. *Int. J. Remote Sens.* **1996**, *17*, 1425–1432. [[CrossRef](#)]
26. Gao, B.C. NDWI—A normalized difference water index for remote sensing of vegetation liquid water from space. *Remote Sens. Environ.* **1996**, *8*, 257–266. [[CrossRef](#)]
27. Xu, H.Q. Modification of normalized difference water index (NDWI) to enhance open water features in remotely sensed imagery. *Int. J. Remote Sens.* **2006**, *27*, 3025–3033. [[CrossRef](#)]
28. Tucker, C.J. Remote Sensing of Leaf Water Content in the Near Infrared. *Remote Sens. Environ.* **1980**, *10*, 23–32. [[CrossRef](#)]
29. Quirós, R.; Drago, E. The environmental state of Argentinean lakes: An overview. *Lakes Reserv. Res. Manag.* **1999**, *4*, 55–64. [[CrossRef](#)]

30. Valladares, A. *Cuenca de los ríos Senguer y Chico*; Technical Report; Subsecretaría de Recursos Hídricos de la Nación: Buenos Aires, Argentina, 2004; pp. 1–6.
31. Scordo, F.; Seitz, C.; Zilio, M.; Melo, W.D.; Piccolo, M.C.; Perillo, G.M.E. Evolución de los Recursos Hídricos en el “Bajo de Sarmiento” (Patagonia Extra Andina): Impactos Naturales y Antrópico. *Anu. Inst. Geociênc.* **2017**, *40*, 106–117. [[CrossRef](#)]
32. Dore, M.H.I. Climate change and changes in global precipitation patterns: What do we know? *Environ. Int.* **2005**, *31*, 1167–1181. [[CrossRef](#)] [[PubMed](#)]
33. Compagnucci, R.H.; Araneo, D.C. Alcances de El Niño como predictor del caudal de los ríos andinos argentinos. *Ing. Hidraul. Mex.* **2007**, *22*, 23–35. (In Spanish)
34. Araneo, D.C.; Compagnucci, R.H. Atmospheric circulation features associated to Argentinean Andean rivers discharge variability. *Geophys. Res. Lett.* **2008**, *35*, L01805. [[CrossRef](#)]
35. Masiokas, M.; Villalba, R.; Luckman, B.; Lascano, M.; Delgado, S.; Stepanek, P. 20th-century glacier recession and regional hydroclimatic changes in northwestern Patagonia. *Glob. Planet. Chang.* **2008**, *60*, 85–100. [[CrossRef](#)]
36. Pasquini, A.I.; Lecomte, K.L.; Depetris, P.J. Climate change and recent water level variability in Patagonian proglacial lakes, Argentina. *Glob. Planet. Chang.* **2008**, *63*, 290–298. [[CrossRef](#)]
37. Tejedó, A.G. Degradación de suelos en los alrededores del lago Colhué Huapí, Escalante, provincia de Chubut. In *Primer Congreso de la Ciencia Cartográfica y VII Semana Nacional de la Cartografía*; Centro Argentino de Cartografía: Buenos Aires, Argentina, 2003.
38. Llanos, E.; Behr, S.; Gonzalez, J.; Colombani, E.; Buono, G.; Escobar, J.M. *Informe de las Variaciones del Lago Colhue Huapi Mediante Sensores Remotos y su Relación con las Precipitaciones*; Technical Report; Instituto Nacional de Tecnología Agropecuaria: Trelew, Argentina, 2016; pp. 1–8.
39. Del Valle, H.F.; Elissalde, N.O.; Gagliardini, D.A.; Milovich, J. Status of desertification in the Patagonian region: Assessment and mapping from satellite imagery. *Arid Soil Res. Rehabil.* **1998**, *12*, 95–121.
40. Quirós, R.; Baigun, C.R.M.; Cuch, S.; Delfino, R.; De Nichilo, A.; Guerrero, C.A.; Marinone, M.C.; Menu-Marque, S.A.; Scapini, M.C. *Evaluación del Rendimiento Pesquero Potencial de la República Argentina I: Datos 1*; Technical Report; Departamento de Aguas Continentales, Instituto Nacional de Investigación y Desarrollo Pesquero: Mar del Plata, Argentina, 1988; pp. 1–55.
41. Pedrozo, F.; Childrud, S.; Temporetti, P.; Diaz, M. Chemical composition and nutrient limitation in rivers and lakes of Northern Patagonian Andes (39.5–42° S; 71° W) (Rep. Argentina). *Verh. Int. Verein. Theor. Limnol.* **1993**, *25*, 207–214. [[CrossRef](#)]
42. Diaz, M.; Pedrozo, F.; Reynolds, C.; Temporetti, P. Chemical composition and the nitrogen-regulated trophic state of Patagonian lakes. *Limnologica* **2007**, *37*, 17–27. [[CrossRef](#)]
43. Pérez, G.L.; Torremorell, A.; Bustingorry, J.; Escaray, R.; Pérez, P.; Dieguez, M.; Zagarese, H. Optical characteristics of shallow lakes from the Pampa and Patagonia regions of Argentina. *Limnologica* **2010**, *40*, 30–39. [[CrossRef](#)]
44. Balseiro, E.; Modenutti, B.; Queimaliños, C.; Reissig, M. *Daphnia* distribution in Andean Patagonian lakes: Effect of low food quality and fish predation. *Aquat. Ecol.* **2007**, *41*, 599–609. [[CrossRef](#)]
45. Callieri, C.; Modenutti, B.; Queimalinos, C.; Bertoni, R. Production and biomass of picophytoplankton and larger autotrophs in Andean ultraoligotrophic lakes: Differences in light harvesting efficiency in deep layers. *Aquat. Ecol.* **2007**, *41*, 511–523. [[CrossRef](#)]
46. Izaguirre, I.; Saad, J.F. Phytoplankton from natural water bodies of the Patagonian Plateau. *Advanc. Limnol.* **2014**, *65*, 309–319. [[CrossRef](#)]
47. González Díaz, E.F.; Di Tommaso, I. Paleogeofomas lacustres en los lagos Musters y Colhué Huapí, su relación genética con un paleolago Sarmiento previo, centro sur del Chubut. [Paleo lacustrine landforms in Colhué Huapí and Musters lakes, their genetic connection with a previous Sarmiento paleolake, Central-South Chubut]. *Rev. Asoc. Geol. Argentina* **2014**, *71*, 416–426.
48. Bruniard, E.D. *Hidrografía: Procesos y Tipos de Esgurrimiento Superficial*; Editorial Ceyne: Buenos Aires, Argentina, 1992; pp. 1–124. ISBN 950-9871-25-7.
49. (SSRH) Subsecretaría de Recursos Hídricos de la Nación Argentina. Publicaciones Hidrometeorológicas. 2014. Available online: <https://www.mininterior.gov.ar/obras-publicas/hidro-publicaciones.php> (accessed on 15 December 2017).

50. Coronato, A.; Mazzoni, E.; Vázquez, M.; Coronato, F. *Patagonia: Una Síntesis de su Geografía Física*; Universidad Nacional de la Patagonia Austral: Río Gallegos, Argentina, 2017; pp. 1–217. ISBN 978-987-3714-40-5.
51. Duda, R.D.; Hart, P.E.; Stork, D.G. *Pattern Classification and Scene Analysis*, 2nd ed.; John Wiley & Sons Inc.: New York, NY, USA, 1995; pp. 1–69.
52. Chuvieco Salinero, E. *Teledetección Ambiental. La Observación de la Tierra Desde el Espacio*; Editorial Ariel S.A.: Barcelona, Spain, 2010; pp. 1–582. ISBN 8434434989.
53. Olmanson, L.G.; Bauer, M.E.; Brezonik, P.L. A 20-year Landsat water quality census of Minnesota's 10,000 lakes. *Remote Sens. Environ.* **2008**, *112*, 4086–4097. [[CrossRef](#)]
54. Reis, S.; Yilmaz, H.M. Temporal monitoring of water level changes in Seyfe lake using remote sensing. *Hydrol. Proc.* **2008**, *22*, 4448–4457. [[CrossRef](#)]
55. El-Hattab, M.M. Applying post classification change detection technique to monitor an Egyptian coastal zone (Abu Qir Bay). *Egypt. J. Remote Sens. Space Sci.* **2016**, *19*, 23–36. [[CrossRef](#)]
56. Doña, C.; Chang, N.; Caselles, V.; Sánchez, J.M.; Pérez-Planells, L.; del Bisquert, M.M.; García-Santos, V.; Imen, S.; Camacho, A. Monitoring Hydrological Patterns of Temporary Lakes Using Remote Sensing and Machine Learning Models: Case Study of La Mancha Húmeda Biosphere Reserve in Central Spain. *Remote Sens.* **2016**, *8*, 618. [[CrossRef](#)]
57. Ji, L.; Zhang, L.; Wylie, B. Analysis of Dynamic Thresholds for the Normalized Difference Water Index. *Photogramm. Eng. Remote Sens.* **2009**, *75*, 1307–1317. [[CrossRef](#)]
58. Lyons, E.A.; Sheng, Y.; Smith, L.C.; Li, J.; Hinkel, K.M.; Lenters, J.D.; Wang, J. Quantifying sources of error in multitemporal multisensor lake mapping. *Int. J. Remote Sens.* **2013**, *34*, 7887–7905. [[CrossRef](#)]



© 2018 by the authors. Licensee MDPI, Basel, Switzerland. This article is an open access article distributed under the terms and conditions of the Creative Commons Attribution (CC BY) license (<http://creativecommons.org/licenses/by/4.0/>).